Open access • Proceedings Article • DOI:10.1109/GLOCOM.2011.6133561

Closed-Form Error Probability of Network-Coded Cooperative Wireless Networks with Channel-Aware Detectors — Source link

Michela Iezzi, Marco Di Renzo, Fabio Graziosi

Institutions: University of L'Aquila

Published on: 01 Dec 2011 - Global Communications Conference

Topics: Wireless network, Linear network coding, Relay, Decoding methods and Redundancy (engineering)

Closed-Form Error Probability of Network-Coded Cooperative Wireless Networks with Channel-Aware Detectors

Michela Iezzi, Marco Di Renzo, Fabio Graziosi

Closed–Form Error Probability of Network–Coded Cooperative Wireless Networks with Channel–Aware Detectors

Michela Iezzi[(1)], Marco Di Renzo[(2)], Fabio Graziosi[(1)]
[(1)] University of L'Aquila, College of Engineering
Department of Electrical and Information Engineering (DIEI), Center of Excellence of Research DEWS
Via G. Gronchi 18, Nucleo Industriale di Pile, 67100 L'Aquila, Italy
[(2)] L2S, UMR 8506 CNRS – SUPELEC – Univ Paris–Sud
Laboratory of Signals and Systems (L2S), French National Center for Scientific Research (CNRS)
École Supérieure d'Électricité (SUPÉLEC), University of Paris–Sud XI (UPS)
3 rue Joliot–Curie, 91192 Gif–sur–Yvette (Paris), France
E–Mail: marco.direnzo@lss.supelec.fr, {michela.iezzi, fabio.graziosi}@univaq.it

***Abstract*— In this paper, we propose a simple analytical methodology to study the performance of multi–source multi–relay cooperative wireless networks with network coding at the relay nodes and Maximum–Likelihood (ML–) optimum channel–aware detectors at the destination. Channel–aware detectors are a broad class of receivers that account for possible decoding errors at the relays, and, thus, are inherently designed to mitigate the effect of erroneous forwarded and network–coded data. In spite of the analytical complexity of the problem at hand, the proposed framework turns out to be simple enough yet accurate and insightful to understand the behavior of the system, and, in particular, to capture advantages and disadvantages of various network codes and the impact of error propagation on their performance. It is shown that, with the help of cooperation, some network codes are inherently more robust to decoding errors at the relays, while others better exploit the inherent spatial diversity and redundancy provided by cooperative networking. Finally, theory and simulation highlight that the relative advantage of a network code with respect to the others might be different with and without decoding errors at the relays.**

I. Introduction

Cooperative communications and network coding have recently emerged as strong candidate technologies for many future wireless applications, such as cellular networks, wireless sensor networks, fixed broadband wireless systems, and vehicular networks. Since their inception in [1] and [2], they have been extensively studied to improve the performance of wireless networks. In particular, theory and experiments have shown that they can be extremely useful for wireless networks with disruptive channel and connectivity conditions [3], [4].

However, similar to many other technologies, multi–hop/cooperative communications and network coding are not without limitations [5]. More specifically, relay transmissions consume extra bandwidth resources, which implies that using cooperative diversity typically results in a loss of system throughput. On the other hand, network coding might be very susceptible to transmission errors caused by noise, fading, or interference. In fact, the algebraic operations accomplished by intermediate nodes of the network introduce some packet dependencies in a way that the injection of even a single erroneous packet has the potential to corrupt every packet received by the destination. In the light of their own advantages and limitations, it seems very natural to jointly exploit cooperation and network coding to better take advantage and retain their key benefits while overcoming their limitations. For example, network coding can be an effective enabler to recover the throughput loss experienced by multi–hop/cooperative communications, while the redundancy inherently provided by cooperation might significantly help to alleviate the error propagation problem that arises when mixing the packets.

In this context, the fundamental issue to be accounted for to understand the actual performance improvement and advantage of network–coded cooperative communications is to carefully consider that all the nodes of the network are error–prone, and that erroneous decoding and forwarding might have a significant impact on the end–to–end performance, diversity, throughput, and quality–of–service. The conventional method that is often advocated as a solution to counteract the error propagation problem is the adoption of a Cyclic Redundancy Code (CRC) check mechanism at the relays, which aims at not forwarding corrupted packets [6]. However, recent results have shown by simulation that, in addition to be highly spectral inefficient as an entire packet is blocked if just one bit is in error, relaying based on CRC check might not be very effective in block–fading channels [7].

Because of its well–acknowledged importance in network–coded multi–hop/cooperative networks, how to tackle the error propagation problem has recently attracted the interest of many researchers, and some latest results on the matter are available with and without network coding in [6]–[11] and references therein. More specifically, two classes of solutions have recently emerged: threshold–based relaying (see, *e.g.*, [6], [7]) and channel–aware detectors at the destination (see, *e.g.*, [8], [10], [11]). Due to space constraints, a careful review of all the contributions is not possible here, and the interested readers are kindly requested to consult the references above for further details. In this paper, we will focus our attention only on the latter family of solutions. In particular, channel–aware receivers let the relay nodes forwarding all the received data without necessarily checking their reliability. On the other hand, the destination takes advantage of Channel State Information (CSI) of the overall network to optimally process all the received data according to the instantaneous quality of each wireless link. Recent results have shown that these receivers can fully–exploit the diversity provided by cooperation without [8] and with [11] network coding, respectively. However, it is well–known that these receivers are extremely difficult to be studied analytically, which prevents us to get a clear understanding of their performance, to enable a simple comparison among various solutions without resorting to time–consuming simulations, and to perform system optimization. A survey of the complexity of modeling these detectors can be found in [8], [11], and references therein.

Motivated by these considerations, in this paper we aim at providing a simple yet accurate and, more important, insightful analytical framework to compute the Average Bit Error

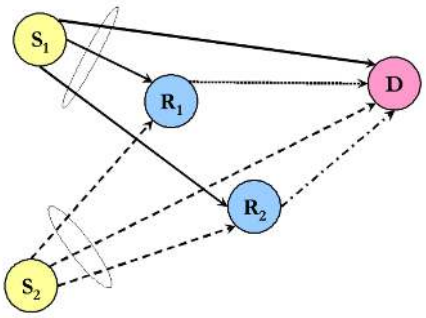

Fig. 1. Two–source two–relay network topology. Different line–styles denote transmission over orthogonal channels (*e.g.*, time–slots) to avoid mutual interference: S_1 transmits in time–slot 1 (solid lines), S_2 in time–slot 2 (dashed lines), R_1 in time–slot 3 (dotted lines), and R_2 in time–slot 4 (dashed–dotted lines).

Probability (ABEP) of network–coded cooperative wireless networks with channel–aware detectors. In particular, our main objective is twofold: i) to enable a simple comparison of various network codes and to study their achievable diversity when used in a cooperative networking scenario, and ii) to understand the impact of decoding errors at the relays for each of them. This paper represents a substantial extension of our previous work [11], where we were able to compute closed–form expressions of the ABEP of channel–aware detectors only for ideal source–to–relay channels, *i.e.*, by neglecting the error propagation effect. As mentioned in [8] for cooperative networks, this is a very difficult analytical problem, which is here shown to become even more complicated when network coding is taken into account. However, we exploit simple approximations to get asymptotically–tight estimates.

The paper is organized as follows. In Section II, system model, network code, and receiver design are introduced. In Section III, the analytical framework to compute the ABEP of the proposed channel–aware detector with non–ideal source–to–relay channels is described. In Section IV, high–SNR (Signal–to–Noise–Ratio) analysis is performed, and diversity and coding gains of four network codes are compared. In Section V, some numerical results are shown. Finally, Section VI concludes the paper.

II. System Model

We consider the canonical two–source two–relay cooperative network in Fig. 2. In time slot $t = 1, 2$, source node S_t broadcasts a modulated symbol, x_{S_t}, with average energy E_m. By assuming uncoded Binary Phase Shift Keying (BPSK) modulation, we have $x_{S_t} = \sqrt{E_m}\,(1 - 2b_{S_t})$, where $b_{S_t} \in \{0, 1\}$ is the bit emitted by S_t. Thus, the bits received at relays R_1, R_2, and destination D, respectively, are:

$$\begin{cases} y_{S_tR_1} = h_{S_tR_1} x_{S_t} + n_{S_tR_1} \\ y_{S_tR_2} = h_{S_tR_2} x_{S_t} + n_{S_tR_2} \\ y_{S_tD} = h_{S_tD} x_{S_t} + n_{S_tD} \end{cases} \tag{1}$$

where h_{XY} is the fading coefficient from node X to node Y, which is a circular symmetric complex Gaussian Random Variable (RV) with zero mean and variance σ^2_{XY} per dimension (Rayleigh fading). For analytical tractability, independent and identically distributed (i.i.d.) fading over all the wireless links is considered, *i.e.*, $\sigma_0^2 = \sigma^2_{XY}$ for any X and Y. Furthermore, n_{XY} is the complex Additive White Gaussian Noise (AWGN) at the input of node Y and related to the transmission from node X to node Y. The AWGN in different time slots is i.i.d. with zero mean and variance $N_0/2$ per dimension.

Notation. The following notation is used: i) $\bar{\gamma} = 2E_m/N_0$; ii) $Q(x) = \left(1/\sqrt{2\pi}\right) \int_x^{+\infty} \exp\left(-t^2/2\right) dt$ is the Q–function; iii) $P_{XY} = Q\left(\sqrt{\bar{\gamma}\gamma_{XY}}\right)$ is the BEP over the wireless link from node X to node Y, where $\gamma_{XY} = |h_{XY}|^2$; iv) $\Pr\{\cdot\}$ denotes probability; v) $g_X(\cdot)$ and $G_X(\cdot)$ denote Probability Density Function (PDF) and Cumulative Distributed Function (CDF) of RV X, respectively; vi) $\otimes$ is the convolution operator; vii) $\delta(\cdot)$ is the Dirac delta function; viii) $H(\cdot)$ is the Heaviside step function; ix) $\mathrm{E}\{\cdot\}$ denotes the expectation operator; x) $\mu = \sqrt{\bar{\gamma}\sigma_0^2/(1 + \bar{\gamma}\sigma_0^2)}$; xi) $\bar{P} = (1/2)(1 - \mu)$; and xii) $\oplus$ denotes bit–wise XOR.

A. Relay Operations

Similar to recent works on cooperative diversity without (*e.g.*, [8], [9]) and with (*e.g.*, [7], [10], [11]) network coding, we assume that the relays perform network coding without checking if the packet is correct or wrong by resorting to, *e.g.*, CRC–enabled error detection. Thus, the operation of the relays can be defined as demodulate–network–code–and–forward.

More specifically, the relays perform coherent ML–optimum demodulation as follows ($t = 1, 2$):

$$\begin{cases} \hat{b}_{S_tR_1} = \underset{\tilde{b}_{S_t} \in \{0,1\}}{\arg\min} \left\{ \left| y_{S_tR_1} - \sqrt{E_m} h_{S_tR_1} \left(1 - 2\tilde{b}_{S_t}\right) \right|^2 \right\} \\ \hat{b}_{S_tR_2} = \underset{\tilde{b}_{S_t} \in \{0,1\}}{\arg\min} \left\{ \left| y_{S_tR_2} - \sqrt{E_m} h_{S_tR_2} \left(1 - 2\tilde{b}_{S_t}\right) \right|^2 \right\} \end{cases} \tag{2}$$

where $\hat{\cdot}$ denotes the detected symbol and $\tilde{\cdot}$ denotes the trial symbol used in the hypothesis–detection problem.

After demodulation, each relay R_q: i) performs network coding on the estimated bits, ii) re–modulates the network–coded bit, and iii) transmits the modulated bit to the destination during the third ($q = 1$) and fourth ($q = 2$) time–slot. By denoting with $f_{R_q}(\cdot, \cdot)$ the network coding operation performed by relay R_q, *i.e.*, $b_{R_q} = f_{R_q}\left(\hat{b}_{S_1R_q}, \hat{b}_{S_2R_q}\right)$, the bit received at the destination D is:

$$y_{R_qD} = h_{R_qD} x_{R_q} + n_{R_qD} \tag{3}$$

where $x_{R_q} = \sqrt{E_m}\left(1 - 2b_{R_q}\right)$.

B. Network Codes

Similar to [11], we aim at analyzing and comparing four network codes (or network coding scenarios), which determine the function $b_{R_q} = f_{R_q}(\cdot, \cdot)$: i) *Scenario 1*: $b_{R_1} = \hat{b}_{S_1R_1}$ and $b_{R_2} = \hat{b}_{S_2R_2}$; ii) *Scenario 2*: $b_{R_1} = \hat{b}_{S_1R_1} \oplus \hat{b}_{S_2R_1}$ and $b_{R_2} = \hat{b}_{S_1R_2} \oplus \hat{b}_{S_2R_2}$; iii) *Scenario 3*: $b_{R_1} = \hat{b}_{S_1R_1} \oplus \hat{b}_{S_2R_1}$ and $b_{R_2} = \hat{b}_{S_2R_2}$; and iv) *Scenario 4*: $b_{R_1} = \hat{b}_{S_1R_1}$ and $b_{R_2} = \hat{b}_{S_1R_2} \oplus \hat{b}_{S_2R_2}$. Further details about the rational for these network codes are available in [11].

The methodology for performance analysis we introduce in Section III is applicable to all the network codes above. However, due to space constraints and for ease of description, in Section II-C and in Section III we focus our attention only on *Scenario 4*. On the other hand, in Section IV we summarize, for high–SNRs, the ABEP of all the network codes, which allows us to compare them in a simple way. The frameworks are substantiated via Monte Carlo simulations in Section V.

C. Receiver Operations

As mentioned in Section I, we are interested in analytically studying the performance of channel–aware detectors, which are based on the Maximum Likelihood Sequence Estimation (MLSE) criterion of optimality with hard–decision decoding at the physical layer. More specifically, given y_{S_1D}, y_{S_2D}, y_{R_1D}, y_{R_2D}, the analyzed detector encompasses two main steps [11]:

$$\begin{aligned}\mathrm{PEP}\left(\mathbf{c}^{(1)}\to\mathbf{c}^{(3)}\right) &= \Psi_1\Psi_3\Psi_4 H\left(w_1+w_3+w_4\right)+\left(1-\Psi_1\right)\left(1-\Psi_3\right)\left(1-\Psi_4\right)H\left(-w_1-w_3-w_4\right)+\left(1-\Psi_1\right)\left(1-\Psi_3\right)\Psi_4 H\left(-w_1-w_3+w_4\right)\\ &+\left(1-\Psi_1\right)\Psi_3\left(1-\Psi_4\right)H\left(-w_1+w_3-w_4\right)+\Psi_1\left(1-\Psi_3\right)\left(1-\Psi_4\right)H\left(w_1-w_3-w_4\right)+\left(1-\Psi_1\right)\Psi_3\Psi_4 H\left(-w_1+w_3+w_4\right)\\ &+\Psi_1\left(1-\Psi_3\right)\Psi_4 H\left(w_1-w_3+w_4\right)+\Psi_1\Psi_3\left(1-\Psi_4\right)H\left(w_1+w_3-w_4\right)\\ &\overset{(a)}{\approx}\Psi_1\Psi_3\Psi_4\\ &+\Psi_1 H\left(w_1-w_3-w_4\right)+\Psi_3\Psi_4 H\left(-w_1+w_3+w_4\right)\leftarrow\Upsilon_1^{(3,4)}\\ &+\Psi_3 H\left(-w_1+w_3-w_4\right)+\Psi_1\Psi_4 H\left(w_1-w_3+w_4\right)\leftarrow\Upsilon_3^{(1,4)}\\ &+\Psi_4 H\left(-w_1-w_3+w_4\right)+\Psi_1\Psi_3 H\left(w_1+w_3-w_4\right)\leftarrow\Upsilon_4^{(1,3)}\end{aligned}\tag{9}$$

a) Step 1 (Physical Layer): Hard–decision estimates of $[b_{S_1}, b_{S_2}, b_{R_1}, b_{R_2}]$ are provided by using a ML–optimum receiver with full–CSI about the source–to–destination and relay–to–destination channels ($t = 1, 2$ and $q = 1, 2$):

$$\begin{cases}\hat{b}_{S_tD} = \underset{\tilde{b}_{S_t}\in\{0,1\}}{\arg\min}\left\{\left|y_{S_tD}-\sqrt{E_m}h_{S_tD}\left(1-2\tilde{b}_{S_t}\right)\right|^2\right\}\\ \hat{b}_{R_qD} = \underset{\tilde{b}_{R_q}\in\{0,1\}}{\arg\min}\left\{\left|y_{R_qD}-\sqrt{E_m}h_{R_qD}\left(1-2\tilde{b}_{R_q}\right)\right|^2\right\}\end{cases}\tag{4}$$

b) Step 2 (Network Layer): The hard–decision estimates $\hat{\mathbf{c}} = [\hat{c}_1, \hat{c}_2, \hat{c}_3, \hat{c}_4] = \left[\hat{b}_{S_1D}, \hat{b}_{S_2D}, \hat{b}_{R_1D}, \hat{b}_{R_2D}\right]$ are input to the network layer, which uses a MLSE–optimum decoder [12] with full–CSI to retrieve the bits emitted by the sources:

$$\left[\hat{b}_{S_1}, \hat{b}_{S_2}\right] = \left[c_1^{(\hat{j})}, c_2^{(\hat{j})}\right] = \underset{\mathbf{c}^{(\tilde{j})}\text{ with }\tilde{j}=1,2,3,4}{\arg\min}\left\{\sum_{i=1}^{4} w_i\left|\hat{c}_i - c_i^{(\tilde{j})}\right|\right\}\tag{5}$$

where, as far as *Scenario 4* is concerned, we have: i) $w_i = \ln\left[(1-\Psi_i)/\Psi_i\right]$; ii) $\Psi_1 = P_{S_1D}$, $\Psi_2 = P_{S_2D}$, $\Psi_3 = P_{S_1R_1} + P_{R_1D} - 2P_{S_1R_1}P_{R_1D}$, and $\Psi_4 = P_{R_2D} + P_{S_1R_2} + P_{S_2R_2} - 2P_{S_1R_2}P_{S_2R_2} - 2P_{R_2D}\left(P_{S_1R_2} + P_{S_2R_2} - 2P_{S_1R_2}P_{S_2R_2}\right)$; and iii) $c_i^{(j)}$ is the i–th element of $\mathbf{c}^{(j)}$, which is the j–th codeword of the codebook $\mathcal{C} = \left\{\mathbf{c}^{(1)}, \mathbf{c}^{(2)}\mathbf{c}^{(3)}, \mathbf{c}^{(4)}\right\} = \{0000, 0101, 1011, 1110\}$.

III. Closed–Form Computation of the ABEP

By direct inspection of the codebook $\mathcal{C}$ of *Scenario 4* and from (5), the ABEP of S_1 and S_2 can be computed as:

$$\begin{cases}\mathrm{ABEP}_{S_1} = \mathrm{APEP}\left(\mathbf{c}^{(1)}\to\mathbf{c}^{(3)}\right)+\mathrm{APEP}\left(\mathbf{c}^{(1)}\to\mathbf{c}^{(4)}\right)\\ \mathrm{ABEP}_{S_2} = \mathrm{APEP}\left(\mathbf{c}^{(1)}\to\mathbf{c}^{(2)}\right)+\mathrm{APEP}\left(\mathbf{c}^{(1)}\to\mathbf{c}^{(4)}\right)\end{cases}\tag{6}$$

where $\mathrm{APEP}\left(\mathbf{c}^{(1)}\to\mathbf{c}^{(j)}\right)$ for $j = 2, 3, 4$ is the Average (over fading channel statistics) Pairwise Error Probability (APEP), *i.e.*, $\mathrm{APEP}\left(\mathbf{c}^{(1)}\to\mathbf{c}^{(3)}\right) = \mathrm{E}\left\{\mathrm{PEP}\left(\mathbf{c}^{(1)}\to\mathbf{c}^{(3)}\right)\right\}$, and:

$$\begin{aligned}\mathrm{PEP}\left(\mathbf{c}^{(1)}\to\mathbf{c}^{(j)}\right) &= \Pr\left\{D^{(1)} > D^{(j)}\right\}\\ &= \Pr\left\{\sum_{i=1}^{4} w_i\left|\hat{c}_i - c_i^{(1)}\right| > \sum_{i=1}^{4} w_i\left|\hat{c}_i - c_i^{(j)}\right|\right\}\end{aligned}\tag{7}$$

The computation of $\mathrm{APEP}\left(\mathbf{c}^{(1)}\to\mathbf{c}^{(j)}\right)$ is almost the same for $j = 2, 3, 4$. Thus, for the sake of concision, we report the analytical derivation only for $\mathrm{APEP}\left(\mathbf{c}^{(1)}\to\mathbf{c}^{(3)}\right)$.

A. Computation of $\mathrm{PEP}\left(\mathbf{c}^{(1)}\to\mathbf{c}^{(3)}\right)$

By introducing the RV $D^{(1,3)} = D^{(1)} - D^{(3)} = \sum_{i=1}^{4} d_i^{(1,3)}$ with $d_i^{(1,3)} = w_i\left[\left|\hat{c}_i - c_i^{(1)}\right| - \left|\hat{c}_i - c_i^{(3)}\right|\right]$, the $\mathrm{PEP}\left(\mathbf{c}^{(1)}\to\mathbf{c}^{(3)}\right)$ can be explicitly written as:

$$\mathrm{PEP}\left(\mathbf{c}^{(1)}\to\mathbf{c}^{(3)}\right) = \Pr\left\{D^{(1,3)} > 0\right\} = \int_0^{+\infty} g_{D^{(1,3)}}(\xi)\, d\xi\tag{8}$$

The PDF, $g_{D^{(1,3)}}(\cdot)$, of RV $D^{(1,3)}$, can be computed analytically from the following considerations: i) $D^{(1,3)}$ is the summation of four RVs, *i.e.*, $d_i^{(1,3)}$ for $i = 1, 2, 3, 4$; ii) the RVs $d_i^{(1,3)}$ are independent because relays and destination work independently and receive the signals in non–overlapping time–slots; and iii) from (4), it follows that $\hat{c}_i$ for $i = 1, 2, 3, 4$ are four Bernoulli–distributed RVs with PDF given by $g_{\hat{c}_i}(\xi) = (1-\Psi_i)\,\delta(\xi) + \Psi_i\,\delta(\xi-1)$. Accordingly, we obtain $g_{D^{(1,3)}}(\xi) = \left(g_{d_1^{(1,3)}} \otimes g_{d_2^{(1,3)}} \otimes g_{d_3^{(1,3)}} \otimes g_{d_4^{(1,3)}}\right)(\xi)$, where $g_{d_i^{(1,3)}}(\xi) = (1-\Psi_i)\,\delta(\xi+w_i) + \Psi_i\,\delta(\xi-w_i)$ for $i = 1, 3, 4$ and $g_{d_2^{(1,3)}}(\xi) = \delta(\xi)$. Thus, by substituting $g_{D^{(1,3)}}(\cdot)$ in (8) and exploiting the properties of the Dirac delta function, we obtain, after some algebra, the PEP in (9) on top of this page. In particular, in $\overset{(a)}{\approx}$ we have taken into account that (for $i = 1, 2, 3, 4$): i) $H(w_1 + w_3 + w_4) = 1$ and $H(-w_1 - w_3 - w_4) = 0$ since $w_i > 0$; and ii) $1 - \Psi_i \approx 1$ for high–SNRs, *i.e.*, when $\Psi_i \ll 1$.

Finally, from the definition of w_i in Section II-C, (9) can be shown to be equivalent to:

$$\begin{aligned}\mathrm{PEP}\left(\mathbf{c}^{(1)}\to\mathbf{c}^{(3)}\right) &= \Psi_1\Psi_3\Psi_4\\ &+\underbrace{\min\left\{\Psi_1, \Psi_3\Psi_4\right\}}_{\Upsilon_1^{(3,4)}}+\underbrace{\min\left\{\Psi_3, \Psi_1\Psi_4\right\}}_{\Upsilon_3^{(1,4)}}+\underbrace{\min\left\{\Psi_4, \Psi_1\Psi_3\right\}}_{\Upsilon_4^{(1,3)}}\end{aligned}\tag{10}$$

B. Computation of $\mathrm{APEP}\left(\mathbf{c}^{(1)}\to\mathbf{c}^{(3)}\right)$

The next step is to remove the conditioning over fading channel statistics, *i.e.*, computing $\mathrm{APEP}\left(\mathbf{c}^{(1)}\to\mathbf{c}^{(3)}\right) = \mathrm{E}\left\{\mathrm{PEP}\left(\mathbf{c}^{(1)}\to\mathbf{c}^{(3)}\right)\right\}$. From (10), we have:

$$\begin{aligned}\mathrm{APEP}\left(\mathbf{c}^{(1)}\to\mathbf{c}^{(3)}\right) &= \mathrm{E}\left\{\Psi_1\right\}\mathrm{E}\left\{\Psi_3\right\}\mathrm{E}\left\{\Psi_4\right\}\\ &+\mathrm{E}\left\{\Upsilon_1^{(3,4)}\right\}+\mathrm{E}\left\{\Upsilon_3^{(1,4)}\right\}+\mathrm{E}\left\{\Upsilon_4^{(1,3)}\right\}\end{aligned}\tag{11}$$

Under the assumption of i.i.d. Rayleigh fading (see Section II), $\mathrm{E}\{\Psi_i\}$ for $i = 1, 3, 4$ can be computed in closed–form as $\mathrm{E}\{\Psi_1\} = \bar{P}$, $\mathrm{E}\{\Psi_3\} = 2\bar{P} - 2\bar{P}^2$, and $\mathrm{E}\{\Psi_4\} = 3\bar{P} - 6\bar{P}^2 + 4\bar{P}^3$. On the other hand, the exact computation of $\bar{\Upsilon}_1^{(3,4)} = \mathrm{E}\left\{\Upsilon_1^{(3,4)}\right\}$, $\bar{\Upsilon}_3^{(1,4)} = \mathrm{E}\left\{\Upsilon_3^{(1,4)}\right\}$, and $\bar{\Upsilon}_4^{(1,3)} = \mathrm{E}\left\{\Upsilon_4^{(1,3)}\right\}$ is quite cumbersome. Thus, to get useful and insightful results, we resort to simple but accurate approximations for their computation. Due to space constraints, in this section we focus our attention only on $\bar{\Upsilon}_4^{(1,3)}$, as $\bar{\Upsilon}_1^{(3,4)}$ and $\bar{\Upsilon}_3^{(1,4)}$ can be computed with similar steps.

In particular, Appendix I shows that $\Upsilon_4^{(1,3)}$ can be tightly approximated as follows:

$$\Upsilon_4^{(1,3)} = \min\left\{\Psi_4, \Psi_1\Psi_3\right\} \approx Q\left(\sqrt{\bar{\gamma}\max\left\{\gamma_{3\mathrm{h}}, k_4^{(1,3)}\gamma_{\mathrm{d}-2\mathrm{h}}\right\}}\right)\tag{12}$$

where we have defined: i) $\gamma_{2\mathrm{h}} = \left(\gamma_{S_1R_1}^{-1} + \gamma_{R_1D}^{-1}\right)^{-1}$, ii) $\gamma_{3\mathrm{h}} = \left(\gamma_{S_1R_2}^{-1} + \gamma_{S_2R_2}^{-1} + \gamma_{R_2D}^{-1}\right)^{-1}$, iii) $\gamma_{\mathrm{d}-2\mathrm{h}} = \gamma_{S_1D} + \gamma_{2\mathrm{h}}$, and iv) $k_4^{(1,3)} = \sqrt{3}$. Furthermore, it is worth mentioning that $\gamma_{2\mathrm{h}}$ and $\gamma_{3\mathrm{h}}$ are the end–to–end SNRs of an equivalent two– and three–hop network with ideal channel inversion at the relay [13].

From (12), $\bar{\Upsilon}_4^{(1,3)}$ can be re–written as follows:

$$\begin{aligned}\bar{\Upsilon}_4^{(1,3)} &\approx \mathrm{E}\left\{Q\left(\sqrt{\bar{\gamma}\max\left\{\gamma_{3\mathrm{h}}, k_4^{(1,3)}\gamma_{\mathrm{d}-2\mathrm{h}}\right\}}\right)\right\}\\ &= \frac{1}{\sqrt{2\pi}}\int_0^{+\infty}\exp\left(-\frac{t^2}{2}\right)G_{\gamma_4^{(1,3)}}\left(\frac{t^2}{\bar{\gamma}}\right)dt\end{aligned}\tag{13}$$

$$\bar{\Upsilon}_4^{(1,3)} \approx \frac{1}{2} - \frac{1}{2}\sqrt{\frac{2\sigma_0^2\bar{\gamma}}{6+2\sigma_0^2\bar{\gamma}}} - \sqrt{\frac{2k_4^{(1,3)}\sigma_0^2\bar{\gamma}}{2+2k_4^{(1,3)}\sigma_0^2\bar{\gamma}}} + \frac{1}{2}\sqrt{\frac{2k_4^{(1,3)}\sigma_0^2\bar{\gamma}}{4+2k_4^{(1,3)}\sigma_0^2\bar{\gamma}}} + \sqrt{\frac{2k_4^{(1,3)}\sigma_0^2\bar{\gamma}}{\left(2+6k_4^{(1,3)}\right)+2k_4^{(1,3)}\sigma_0^2\bar{\gamma}}} - \frac{1}{2}\sqrt{\frac{2k_4^{(1,3)}\sigma_0^2\bar{\gamma}}{\left(4+6k_4^{(1,3)}\right)+2k_4^{(1,3)}\sigma_0^2\bar{\gamma}}} \quad (19)$$

$$\bar{\Upsilon}_3^{(1,4)} \approx \frac{1}{2} - \frac{1}{2}\sqrt{\frac{2\sigma_0^2\bar{\gamma}}{4+2\sigma_0^2\bar{\gamma}}} + \frac{1}{4}\sqrt{\frac{2k_3^{(1,4)}\sigma_0^2\bar{\gamma}}{6+2k_3^{(1,4)}\sigma_0^2\bar{\gamma}}} - \frac{3}{4}\sqrt{\frac{2k_3^{(1,4)}\sigma_0^2\bar{\gamma}}{2+2k_3^{(1,4)}\sigma_0^2\bar{\gamma}}} - \frac{1}{4}\sqrt{\frac{2k_3^{(1,4)}\sigma_0^2\bar{\gamma}}{\left(6+4k_3^{(1,4)}\right)+2k_3^{(1,4)}\sigma_0^2\bar{\gamma}}} + \frac{3}{4}\sqrt{\frac{2k_3^{(1,4)}\sigma_0^2\bar{\gamma}}{\left(2+4k_3^{(1,4)}\right)+2k_3^{(1,4)}\sigma_0^2\bar{\gamma}}} \quad (20)$$

$$\bar{\Upsilon}_1^{(3,4)} \approx \frac{1}{2} - \frac{1}{2}\sqrt{\frac{2\sigma_0^2\bar{\gamma}}{2+2\sigma_0^2\bar{\gamma}}} - \frac{3}{2}\sqrt{\frac{2k_1^{(3,4)}\sigma_0^2\bar{\gamma}}{4+2k_1^{(3,4)}\sigma_0^2\bar{\gamma}}} + \sqrt{\frac{2k_1^{(3,4)}\sigma_0^2\bar{\gamma}}{6+2k_1^{(3,4)}\sigma_0^2\bar{\gamma}}} - \sqrt{\frac{2k_1^{(3,4)}\sigma_0^2\bar{\gamma}}{\left(6+2k_1^{(3,4)}\right)+2k_1^{(3,4)}\sigma_0^2\bar{\gamma}}} + \frac{3}{2}\sqrt{\frac{2k_1^{(3,4)}\sigma_0^2\bar{\gamma}}{\left(4+2k_1^{(3,4)}\right)+2k_1^{(3,4)}\sigma_0^2\bar{\gamma}}} \quad (21)$$

where $\gamma_4^{(1,3)} = \max\left\{\gamma_{3\mathrm{h}}, k_4^{(1,3)}\gamma_{\mathrm{d}-2\mathrm{h}}\right\}$, and the last equality comes from, *e.g.*, [14, Eq. (8)].

By exploiting the independence of channel fading, $G_{\gamma_4^{(1,3)}}(\cdot)$ can be re–written as:

$$\begin{aligned} G_{\gamma_4^{(1,3)}}(x) &= \Pr\left\{\max\left\{\gamma_{3\mathrm{h}}, k_4^{(1,3)}\gamma_{\mathrm{d}-2\mathrm{h}}\right\} < x\right\} \\ &= G_{\gamma_{3\mathrm{h}}}(x)\, G_{\gamma_{\mathrm{d}-2\mathrm{h}}}\left(\tfrac{x}{k_4^{(1,3)}}\right) \end{aligned} \quad (14)$$

where $G_{\gamma_{\mathrm{d}-2\mathrm{h}}}(\cdot)$ can be explicitly written as:

$$\begin{aligned} G_{\gamma_{\mathrm{d}-2\mathrm{h}}}(x) &= \Pr\left\{\gamma_{S_1D} + \gamma_{2\mathrm{h}} < x\right\} \\ &= \mathrm{E}_{\gamma_{2\mathrm{h}}}\left\{G_{\gamma_{S_1D}}(x-\xi|\,\gamma_{2\mathrm{h}}=\xi)\right\} \end{aligned} \quad (15)$$

with $G_{\gamma_{S_1D}}(\cdot|\,\gamma_{2\mathrm{h}})$ being the CDF of γ_{S_1D} conditioned on $\gamma_{2\mathrm{h}}$, and $\mathrm{E}_{\gamma_{2\mathrm{h}}}\{\cdot\}$ being the expectation computed only over $\gamma_{2\mathrm{h}}$. In particular, $G_{\gamma_{S_1D}}(\cdot|\,\gamma_{2\mathrm{h}})$ can be computed in closed–form for Rayleigh fading as follows [12]:

$$G_{\gamma_{S_1D}}(x-\xi|\,\gamma_{2\mathrm{h}}=\xi) = \begin{cases} 1-\exp\left(-\frac{x}{2\sigma_0^2}\right)\exp\left(\frac{\xi}{2\sigma_0^2}\right) & \text{if } x>\xi \\ 0 & \text{elsewhere} \end{cases} \quad (16)$$

Thus, from (15) and (16) we have:

$$\begin{aligned} G_{\gamma_{\mathrm{d}-2\mathrm{h}}}(x) &= \textstyle\int_0^{+\infty} G_{\gamma_{S_1D}}(x-\xi|\,\gamma_{2\mathrm{h}}=\xi)\, g_{\gamma_{2\mathrm{h}}}(\xi)\, d\xi \\ &= G_{\gamma_{2\mathrm{h}}}(x) - \exp\left(-\tfrac{x}{2\sigma_0^2}\right)\textstyle\int_0^x \exp\left(\tfrac{\xi}{2\sigma_0^2}\right) g_{\gamma_{2\mathrm{h}}}(\xi)\, d\xi \end{aligned} \quad (17)$$

From (14) and (17), we conclude that to compute (13) we need closed–form expressions of the PDF and the CDF of CSI–assisted multi–hop networks. These functions are available in closed–form for a variety of fading channel models [13]. Among the many possibilities available in the literature, in this paper we find very useful for the subsequent development to resort to the upper bound in [15, Eq. (11)]. In particular, for a n–hop network we have:

$$g_{\gamma_{\mathrm{nh}}}(\xi) \approx \frac{n}{2\sigma_0^2}\exp\left(-\frac{n}{2\sigma_0^2}\right) \text{ and } G_{\gamma_{\mathrm{nh}}}(\xi) \approx 1-\exp\left(-\frac{n}{2\sigma_0^2}\right) \quad (18)$$

Finally, by substituting (18) with $n=2$ in (17), and (18) with $n=3$ in (14), we can solve (13) in closed–form after some algebra. The final result is shown in (19) on top of this page. Likewise, $\bar{\Upsilon}_3^{(1,4)}$ and $\bar{\Upsilon}_1^{(3,4)}$ can be obtained by using the same methodology, as shown in (20) and (21) on top of this page, respectively, where $k_1^{(3,4)} = k_3^{(1,4)} = \sqrt{3}$.

We close this section by mentioning that $\mathrm{APEP}\left(\mathbf{c}^{(1)} \to \mathbf{c}^{(2)}\right)$ and $\mathrm{APEP}\left(\mathbf{c}^{(1)} \to \mathbf{c}^{(4)}\right)$ can be computed with similar analytical steps. However, the analytical derivation is not reported due to space constraints.

IV. Diversity Analysis

The aim of this section is to study and to understand the behavior of the system under analysis for high–SNR (*i.e.*, for $\bar{\gamma} \gg 1$). The main goal is to develop a very simple yet insightful and accurate framework to compare the performance of the network codes in Section II-B, as well as to understand the impact of realistic source–to–relay channels. The asymptotic ABEP, *i.e.*, ABEP_∞, can be obtained by performing Taylor series expansion of all the terms yielding the APEPs in Section III. For example, a tight high–SNR approximation of (19)–(21) can be obtained, after simple but lengthly analytical computations, from the known result:

$$\sqrt{\frac{a\bar{\gamma}}{b+a\bar{\gamma}}} \overset{\bar{\gamma}\gg 1}{\to} 1 - \frac{b}{2a}\bar{\gamma}^{-1} + \frac{3b^2}{8a^2}\bar{\gamma}^{-2} - \frac{5b^3}{16a^3}\bar{\gamma}^{-3} + o\left(\bar{\gamma}^{-3}\right) \quad (22)$$

Due to space constraints, we are unable to report all the details of the derivation. However, in Table I we summarize the final result for all the network codes described in Section II-B, as well as for two case studies: i) ideal source–to–relay–channels, which provides a benchmark (lower–bound) on the achievable performance, as the relays can perfectly decode the received bits and there is no error propagation [11]; and ii) the actual scenario with faded and noisy source–to–relay–channels we have introduced in Section II and studied in Section III, respectively. These results are substantiated in Section V through Monte Carlo simulations.

Even though very simple, the formulas in Table I provide important insights about the system behavior. More specifically, the following conclusions can be drawn. i) As far as ideal source–to–relay channels are concerned, we notice that there is no gain in using XOR–based network coding (*Scenario 2*) with respect to performing just relaying (*Scenario 1*). On the other hand, network coding based on Unequal Error Protection (UEP) coding [11], *i.e.*, *Scenario 3* and *Scenario 4*, provides much better performance for at least one source, which achieves diversity equal to three. Furthermore, the performance of that source is improved without deteriorating the performance of the other source. ii) As far as realistic source–to–relay channels are concerned, we observe that error propagation at the relays produces a slightly different behavior. More specifically, we notice that XOR–based network coding outperforms the scenario when the relays just forward the received bits. In other words, even the simple XOR–based network coding introduces a coding gain. However, the most remarkable result that can be deduced from Table I is that XOR–based network coding is highly robust to the error propagation caused by erroneous decoding at the relays. In fact, by comparing the setups with ideal and realistic source–to–relay channels we notice that the same asymptotic ABEP is achieved. In other words, cooperation and network coding together allow us to offset the potential performance degradation caused by forwarding wrong bits. This result is very

TABLE I

ABEP FOR HIGH–SNR, *i.e.*, $\mathrm{ABEP}_{\infty} = (G_c \bar{\gamma}_{\infty})^{-G_d}$, WHERE G_c AND G_d ARE CODING AND DIVERSITY GAINS, RESPECTIVELY, AND $\bar{\gamma}_{\infty} = 2\sigma_0^2 (E_m/N_0)$.

	Ideal source–to–relay channels		Realistic source–to–relay channels	
	$\mathrm{ABEP}_{\infty}^{(S_1)}$	$\mathrm{ABEP}_{\infty}^{(S_2)}$	$\mathrm{ABEP}_{\infty}^{(S_1)}$	$\mathrm{ABEP}_{\infty}^{(S_2)}$
Scenario 1	$\left[\left(\sqrt{8/3}\right)\bar{\gamma}_{\infty}\right]^{-2}$	$\left[\left(\sqrt{8/3}\right)\bar{\gamma}_{\infty}\right]^{-2}$	$\left[\left(\sqrt{4/3}\right)\bar{\gamma}_{\infty}\right]^{-2}$	$\left[\left(\sqrt{4/3}\right)\bar{\gamma}_{\infty}\right]^{-2}$
Scenario 2	$\left[\left(\sqrt{8/3}\right)\bar{\gamma}_{\infty}\right]^{-2}$	$\left[\left(\sqrt{8/3}\right)\bar{\gamma}_{\infty}\right]^{-2}$	$\left[\left(\sqrt{8/3}\right)\bar{\gamma}_{\infty}\right]^{-2}$	$\left[\left(\sqrt{8/3}\right)\bar{\gamma}_{\infty}\right]^{-2}$
Scenario 3	$\left[\left(\sqrt{8/3}\right)\bar{\gamma}_{\infty}\right]^{-2}$	$\left[\left(\sqrt[3]{32/31}\right)\bar{\gamma}_{\infty}\right]^{-3}$	$\left[\left(\sqrt{8/9}\right)\bar{\gamma}_{\infty}\right]^{-2}$	$\left[\left(\sqrt[3]{8/31}\right)\bar{\gamma}_{\infty}\right]^{-3}$
Scenario 4	$\left[\left(\sqrt[3]{32/31}\right)\bar{\gamma}_{\infty}\right]^{-3}$	$\left[\left(\sqrt{8/3}\right)\bar{\gamma}_{\infty}\right]^{-2}$	$\left[\left(\sqrt[3]{8/31}\right)\bar{\gamma}_{\infty}\right]^{-3}$	$\left[\left(\sqrt{8/9}\right)\bar{\gamma}_{\infty}\right]^{-2}$

interesting as it is obtained without resorting to any error detection or correction mechanisms at the relays. Another important outcome is that, for at least one source, full–diversity is still achieved by exploiting UEP–based network coding. In this case, however, we notice that the performance for realistic source–to–relay channels is slightly worse than for ideal source–to–relay channels. In addition, the price to be paid to let one source achieving diversity three is worse performance for the other source, if compared to XOR–based network coding. In other words, UEP–based network coding design seems to well exploit the principle of cooperation: the nodes in the network cooperate to let some sources achieving the target ABEP at the expense of some performance and power losses for the other nodes. It is important to emphasize that no performance degradation can be noticed for ideal source–to–relay channels. This highlights, once again, the importance of considering realistic propagation and networking operations to properly design the network.

V. NUMERICAL RESULTS – FRAMEWORK VALIDATION

In this section, we provide some numerical results to substantiate analytical frameworks and claims in Section III and Section IV, respectively. A detailed description of the simulation setup is available in Section II, while the simulation parameters can be found in the caption of each figure.

Some examples are shown in Figs. 2–5, where we compare Monte Carlo simulations with the analytical framework in Section III, and the asymptotic analysis in Table I. It is worth mentioning that, even though only *Scenario 4* is considered in Section III, the figures substantiate our analytical derivation for all the other network codes. Furthermore, for the sake of completeness, each figure reports the ABEP for ideal source–to–relay channels too. In fact, even though this setup was studied in [11], no diversity analysis was conducted therein. The numerical examples in Figs. 2–5 substantiate the tightness of the asymptotic frameworks in Table I for this case study as well. Overall, we notice that the proposed frameworks are very accurate for all network codes and case studies. In particular, we can capture both the coding and diversity gains of the cooperative network under analysis. As expected, the framework in Section III is more accurate for low/medium–SNRs than the results in Table I. However, it seems less insightful and less flexible for system optimization. As far the system behavior with respect to the adopted network code or the effect of realistic source–to–relay channels is concerned, the figures confirm findings and conclusions in Section IV.

VI. CONCLUSION

In this paper, we have provided a general yet simple and accurate methodology to compute in closed–form the ABEP of network–coded cooperative networks with realistic wireless fading channels. The methodology is simple enough to be used for various network codes, and provides frameworks that are simple and accurate enough to understand the system behavior, as well as for a possible end–to–end optimization. Monte Carlo simulations have substantiated our theoretical findings, and have shown that some network codes might be more robust than others to the error propagation problem, as well as that there is a trade–off between robustness to errors on the source–to–relay channels and the diversity gain of any active source.

ACKNOWLEDGMENT

This work is supported, in part, by the research projects "GREENET" (PITN–GA–2010–264759), "JNCD4CoopNets" (CNRS – GDR 720 ISIS, France), and "Re.C.O.Te.S.S.C." (PORAbruzzo, Italy).

APPENDIX I
PROOF OF (12)

From (10), by definition we have $\Upsilon_4^{(1,3)} = \min\{\Psi_4, \Psi_1\Psi_3\}$. The tight approximation in (12) can be obtained from the following considerations.

- By carefully looking at the definitions of Ψ_i for $i = 1, 3, 4$ in Section II-C, we can readily notice that: i) Ψ_1 is the error probability of a direct link and cannot be simplified further; ii) Ψ_3 can be seen as the error probability of an equivalent Decode–and–Forward (DF) link related to the S_1–to–R_1 and R_1–to–D wireless links, which can be accurately approximated, for high–SNRs, by an equivalent two–hop Amplify–and–Forward (AF) link, *i.e.*, $\Psi_3 \approx Q\left(\sqrt{\bar{\gamma}\left(\gamma_{S_1R_1}^{-1} + \gamma_{R_1D}^{-1}\right)^{-1}}\right) = Q\left(\sqrt{\bar{\gamma}\gamma_{2\mathrm{h}}}\right)$ [13]; and iii) Ψ_4 can be seen as the error probability of two equivalent concatenated DF links related to the S_1–to–R_2 and S_2–to–R_2 wireless links, as well as this latter equivalent DF link and the R_2–to–D wireless link. The combination of these two equivalent DF links can be accurately approximated by an equivalent three–hop AF link, *i.e.*, $\Psi_4 \approx Q\left(\sqrt{\bar{\gamma}\left(\gamma_{S_1R_2}^{-1} + \gamma_{S_2R_2}^{-1} + \gamma_{R_2D}^{-1}\right)^{-1}}\right) = Q\left(\sqrt{\bar{\gamma}\gamma_{3\mathrm{h}}}\right)$ [13].
- By replacing the Q–function with its weak Chernoff bound ($Q(x) \leq (1/2)\exp\left(-x^2/2\right) < \exp\left(-x^2/2\right)$ [12]), *i.e.*, $Q(x) \sim \exp\left(-x^2/2\right)$, we have $\Psi_1\Psi_3 \approx Q\left(\sqrt{\bar{\gamma}\gamma_{S_1D}}\right)Q\left(\sqrt{\bar{\gamma}\gamma_{2\mathrm{h}}}\right) \sim \exp\left(-(\bar{\gamma}\gamma_{S_1D} + \bar{\gamma}\gamma_{2\mathrm{h}})/2\right) \sim Q\left(\sqrt{\bar{\gamma}\left(\gamma_{S_1D} + \gamma_{2\mathrm{h}}\right)}\right)$. However, the Chernoff bound can well capture only the slope (*i.e.*, diversity gain) of the Q–function but it cannot capture the coding gain, which results in an error. To compensate for this error, we introduce a correction term, $k_4^{(1,3)}$, *i.e.*, $\Psi_1\Psi_3 \approx Q\left(\sqrt{\bar{\gamma}k_4^{(1,3)}\left(\gamma_{S_1D} + \gamma_{2\mathrm{h}}\right)}\right)$.
- The accurate computation of $k_4^{(1,3)}$ is crucial to get a very tight approximation for high–SNRs. The criterion we use to

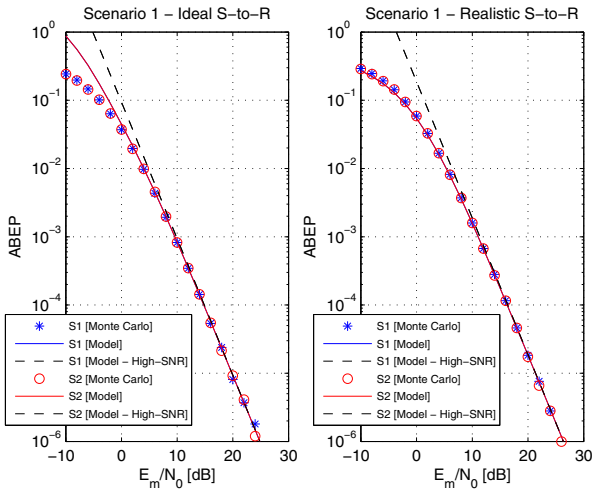

Fig. 2. ABEP against E_m/N_0 for *Scenario 1* ($\sigma_0^2 = 1$).

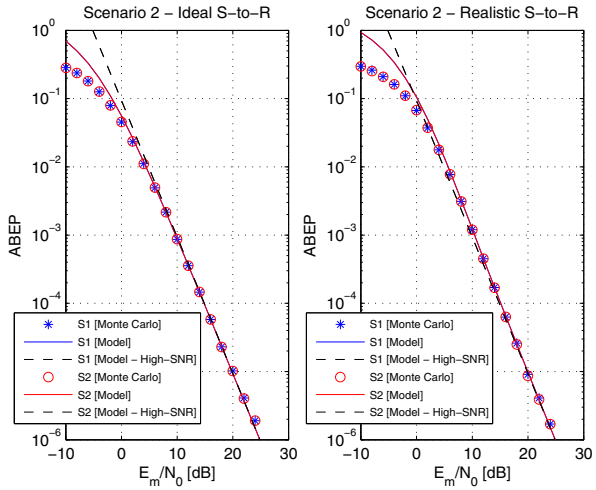

Fig. 3. ABEP against E_m/N_0 for *Scenario 2* ($\sigma_0^2 = 1$).

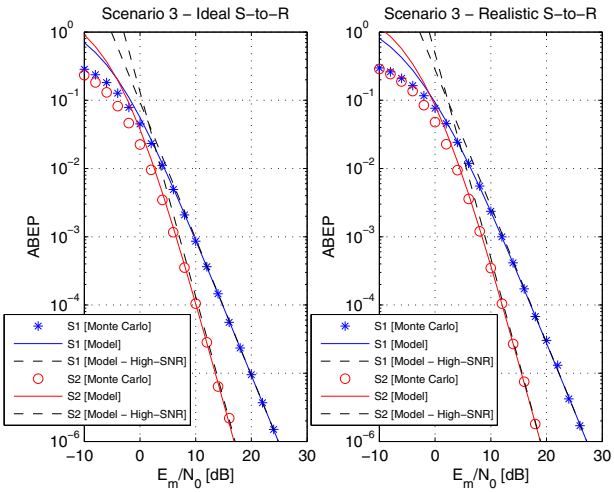

Fig. 4. ABEP against E_m/N_0 for *Scenario 3* ($\sigma_0^2 = 1$).

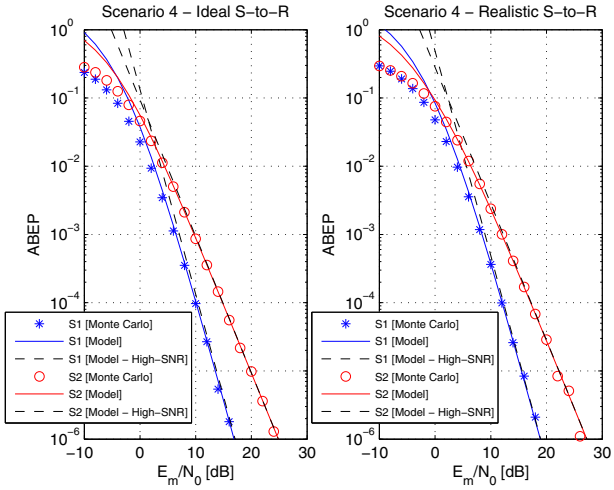

Fig. 5. ABEP against E_m/N_0 for *Scenario 4* ($\sigma_0^2 = 1$).

compute $k_4^{(1,3)}$ is the so–called first–moment–matching, *i.e.*, $k_4^{(1,3)}$ is estimated by imposing, for high–SNRs, the equality $\mathrm{E}\{\Psi_1\Psi_3\} = \mathrm{E}\left\{Q\left(\sqrt{\bar{\gamma}k_4^{(1,3)}\left(\gamma_{S_1D}+\gamma_{2\mathrm{h}}\right)}\right)\right\}$, which turns out to be equivalent to:

$$\mathrm{E}\left\{Q\left(\sqrt{\bar{\gamma}\gamma_{S_1D}}\right)\right\}\mathrm{E}\left\{Q\left(\sqrt{\bar{\gamma}\gamma_{2\mathrm{h}}}\right)\right\} = \mathrm{E}\left\{Q\left(\sqrt{\bar{\gamma}k_4^{(1,3)}\left(\gamma_{S_1D}+\gamma_{2\mathrm{h}}\right)}\right)\right\} \tag{23}$$

which, in turn, by using the high–SNR parametrization in [16], reduces to:

$$\left(4\sigma_0^2\bar{\gamma}\right)^{-1}\left(2\sigma_0^2\bar{\gamma}\right)^{-1} = (3/8)\left(k_4^{(1,3)}\sigma_0^2\bar{\gamma}\right)^{-2} \tag{24}$$

from which we can get $k_4^{(1,3)} = \sqrt{3}$.

- By exploiting the considerations above, $\Upsilon_4^{(1,3)}$ can be re–written as:

$$\begin{aligned}\Upsilon_4^{(1,3)} &\approx \min\left\{Q\left(\sqrt{\bar{\gamma}\gamma_{3\mathrm{h}}}\right), Q\left(\sqrt{\bar{\gamma}k_4^{(1,3)}\left(\gamma_{S_1D}+\gamma_{2\mathrm{h}}\right)}\right)\right\} \\ &= Q\left(\sqrt{\max\left\{\bar{\gamma}\gamma_{3\mathrm{h}}, \bar{\gamma}k_4^{(1,3)}\left(\gamma_{S_1D}+\gamma_{2\mathrm{h}}\right)\right\}}\right)\end{aligned} \tag{25}$$

where the last identity follows by taking into account that the Q–function is monotonically decreasing for increasing values of its argument.

The result in (25) concludes the proof of (12). □

REFERENCES

[1] R. Ahlswede, N. Cai, S.–Y. R. Li, and R. W. Yeung, "Network information flow", *IEEE Trans. Inform. Theory*, vol. 46, no. 4, pp. 1204–1216, July 2000.

[2] J. N. Laneman, D. Tse, and G. Wornell, "Cooperative diversity in wireless networks: Efficient protocols and outage behavior", *IEEE Trans. Inform. Theory*, vol. 50, no. 12, pp. 3062–3080, Dec. 2004.

[3] J.–S. Park, M. Gerla, D. S. Lun, Y. Yi, and M. Medard, "Codecast: A network–coding–based ad hoc multicast protocol", *Wireless Commun.*, vol. 13, no. 5, pp. 76–81, Oct. 2006.

[4] S. Katti, "Network coded wireless architecture", *Ph.D. Dissertation*, Massachusetts Institute of Technology, Sep. 2008.

[5] M. Di Renzo, *et al.*, "Robust wireless network coding – An overview", *Springer Lecture Notes*, LNICST 45, pp. 685–698, 2010.

[6] G. Al–Habian, A. Ghrayeb, M. Hasna, and A. Abu–Dayya, "Threshold–based relaying in coded cooperative networks", *IEEE Trans. Vehicular Technol.*, vol. 60, no. 1, pp. 123–135, Jan. 2011.

[7] S. L. H. Nguyen, A. Ghrayeb, G. Al–Habian, and M. Hasna, "Mitigating error propagation in two–way relay channels with network coding", *IEEE Trans. Wireless Commun.*, vol. 9, no. 11, pp. 3380–3390, Nov. 2010.

[8] M. C. Ju and I–M. Kim, "ML performance analysis of the decode–and–forward protocol in cooperative diversity networks", *IEEE Trans. Wireless Commun.*, vol. 8, no. 7, pp. 3855–3867, July 2009.

[9] D. Liang, S. X. Ng, and L. Hanzo, "Relay–induced error propagation reduction for decode–and–forward cooperative communications", *IEEE GLOBECOM*, pp. 1–5, Dec. 2010.

[10] K. Lee and L. Hanzo, "MIMO–assisted hard versus soft decoding–and-forwarding for network coding aided relaying systems", *IEEE Trans. Wireless Commun.*, vol. 8, no. 1, pp. 376–385, Jan. 2009.

[11] M. Iezzi, M. Di Renzo, and F. Graziosi, "Network code design from unequal error protection coding: Channel–aware receiver design and diversity analysis", *IEEE ICC*, pp. 1–6, June 2011.

[12] J. J. Proakis, *Digital Communications*, McGraw–Hill, 4th ed., 2000.

[13] M. Di Renzo, F. Graziosi, and F. Santucci, "A unified framework for performance analysis of CSI–assisted cooperative communications over fading channels", *IEEE Trans. Commun.*, vol. 57, no. 9, pp. 2552–2557, Sep. 2009.

[14] H. Suraweera and G. K. Karagiannidis, "Closed–form error analysis of the non–identical Nakagami–*m* relay fading channel", *IEEE Commun. Lett.*, vol. 12, no. 4, pp. 259–261, Apr. 2008.

[15] M. O. Hasna, "Average BER of multihop communication systems over fading channels", *IEEE Int. Conf. Elect., Circ. and Syst.*, pp. 723–726, Dec. 2003.

[16] Z. Wang and G. B. Giannakis, "A simple and general parameterization quantifying performance in fading channels", *IEEE Trans. Commun.*, vol. 51, no. 8, pp. 1389–1398, Aug. 2003.